Attention-Tunable Safety Barriers for Human-Autonomy Teaming in Specialized Aviation Missions

Carmen Jimenez Cortes[1], Richard Agbeyibor[2], Jack Kolb[2], Ryan Bowers[2], Karen Feigh[2] and Samuel Coogan[1]

***Abstract*—The integration of autonomous systems into civil and military aviation is shifting crew composition from purely human to collaborative human-autonomy teams. Introducing autonomy enables the implementation of automated safety mechanisms. In this letter, we propose a novel safety barrier that adjusts system behavior based on the operator's attention state. The aggressiveness of the adjustments is tunable, and we propose tuning it based on the measured attention of the human to avoid overly conservative or excessively aggressive behaviors of the system. Our proposed solution is tested in human subject experiments of an Intelligence, Surveillance, and Reconnaissance mission in an immersive flight simulator where attention is measured by tracking the operator's eye gaze. Our experimental results show that the proposed attention-tunable safety barrier improves mission performance compared to a standard control barrier function mechanism.**

***Index Terms*—Safety in HRI, Human Factors and Human-in-the-Loop, and Autonomous Vehicle Navigation**

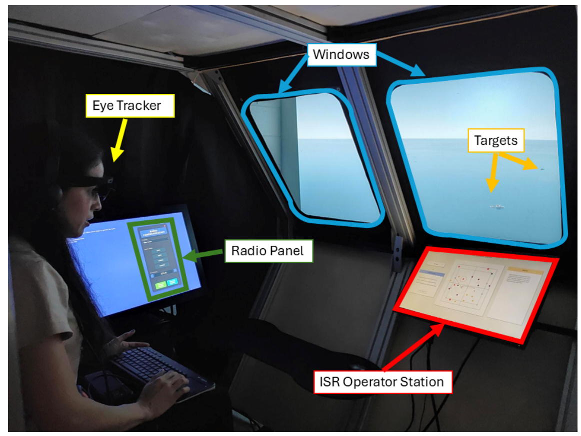

Fig. 1. Immersive Flight Simulator for joint human-AP ISR.

I. Introduction

In many aviation domains, ranging from urban air mobility [1] to military fighter operations [2], research and development is underway to integrate *human-autonomy teaming (HAT)*, in which vehicle control and other critical functions are offloaded to an advanced autonomous pilot (AP) while the human maintains responsibility for high-level decision-making and ultimate mission authority. HAT is often operationalized in aviation as the human operator(s) providing high-level commands, such as desired latitude, longitude and altitude, while the AP executes the piloting tasks to achieve them. Our research explores how various AP control frameworks affect a human-autonomy team's mission performance. Using a flight simulator, we model an Intelligence, Surveillance, and Reconnaissance (ISR) mission, where a joint human–AP team identifies, classifies, and tracks ships in a designated surveillance area. Certain high-threat ships possess weapon employment zones (WEZs) that inflict damage if the aircraft enters them. The operator collaborates with the AP to complete the mission efficiently while avoiding threats. Previous work demonstrated that implementing control barrier functions (CBFs) in this joint human-AP ISR context improved safety but increased mission duration by as much as 20% [3]. This safety performance trade-off is also discussed in [4]. While CBFs reduced the risk of aircraft damage by preventing overflight of high-threat ships, they reduced aircraft speed and lengthened trajectories.

The primary contribution of this letter is the introduction of Attention-Tunable CBFs (AT-CBFs) to mitigate the time-safety trade-off that emerged in previous research. AT-CBFs are inspired by Rate-tunable CBFs [5], which were presented in the context of robotic multi-agent systems, and used trust to adjust the CBF and avoid collisions between agents. In [5], trust is obtained geometrically as a function of both the distance and the angle between agents. In contrast, our proposed AT-CBFs use information about the attention level of the human operator onboard the aircraft to modify the autonomy's behavior. Eye tracking glasses collect operator gaze position, direction, and fixations, and determine gaze location. Based on operator gaze location, the AT-CBF framework relaxes its constraints when the operator is focused on the ISR Operator Station display, and tightens them when their attention shifts elsewhere. The joint human-AP ISR simulator, shown in Figure 1, was inspired by simulators used by the U.S. Navy to train sensor operators for maritime patrol missions [6]. The design process was supervised by a U.S. Navy P-8 ISR pilot, mission commander and instructor. Participants without ISR experience were recruited for the study to resemble new military recruits. Although they are less likely than trained ISR operators to compensate for poor system performance, novice participants impart a few limitations. Their lack of domain expertise may lead to unrepresentative strategies, in-

Manuscript received: March, 18, 2025; Revised June, 17, 2025; Accepted July, 21, 2025.

This paper was recommended for publication by Editor Ki-Uk Kyung upon evaluation of the Associate Editor and Reviewers' comments.

This work was supported by the Office of Naval Research, Science of Autonomy grant N00014-21-1-2759 Human-AI Collaboration in Autonomous Aerial Vehicles.

[1]Carmen Jimenez Cortes and Samuel Coogan are with the School of Electrical and Computer Engineering, Georgia Institute of Technology, Atlanta GA 30332, USA (ccortes9, sam.coogan)@gatech.edu

[2]Richard Agbeyibor, Jack Kolb and Karen Feigh are with the Daniel Guggenheim School of Aerospace Engineering, Georgia Institute of Technology, Atlanta GA 30332, USA (richard.agbeyibor, kolb, rbowers32, karen.feigh)@gatech.edu

Digital Object Identifier (DOI): see top of this page.

flated workload and confounded learning effects. Furthermore, their perception of threat risk may be lower than experienced operators.

The results of a user study with 21 participants confirm that using AT-CBFs as a safety mechanism successfully minimizes damage without extending the duration of the mission, leading to an overall improved mission performance.

The remainder of this letter is structured as follows: Section II presents relevant CBF and HAT literature, while Section III introduces the main notation and definitions. Section IV introduces AT-CBFs, how operator attention is measured and what model is used for its dynamics. Section V describes the specialized ISR aviation mission and the design of the experiment. Section VI presents our results, followed by discussion and the conclusion in Section VII.

II. Related Works

A. Control Barrier Functions

CBFs are a class of control-theoretic tools used to enforce safety in dynamical systems by ensuring that the system's state remains within a predefined safe set. They act as real-time filters or constraints on a controller, intervening only when an action might lead to safety violations. CBFs have been widely applied in safety-critical applications such as autonomous driving [7], legged locomotion [8], and multi-agent coordination [9], where the primary goal is to avoid collisions, or ensure task feasibility under physical and operational constraints. Most existing work on CBFs adopts a standard formulation that enforces safety based on the system's state variables, such as position, velocity, or heading angles, without accounting for human metrics. These methods are well-suited for fully autonomous systems, but they can be overly conservative when applied to shared human-autonomy systems. In such settings, human behavior introduces dynamic uncertainty and adaptation opportunities that are not captured by traditional CBF formulations, leading to potential safety failures or under performance.

B. Human-Autonomy Teaming

Human-machine feedback and adaptive control frameworks have been employed to enhance collaboration between humans and automated, semi-autonomous, and autonomous machines [10]. Physiological feedback such as eye-tracking have been shown to improve mission outcomes in HAT [11]. Specifically, eye gaze (the direction of the operator's visual attention) is a key element [12] in predicting performance, situation awareness (SA) [13], and human-machine interaction, particularly during takeover events [14]. Gaze fixation duration, pupil dilation, and gaze dispersion are common metrics used to assess operator attention and SA [11], [12]. These metrics provide insight into the operator's cognitive state and are crucial for adapting automation in real time. Longer fixation durations on mission-critical displays can indicate focused attention, whereas increased pupil dilation may indicate heightened cognitive load [13]. By incorporating these metrics, autonomous systems can adapt their behavior to support the human more effectively, reducing workload and enhancing mission performance.

C. Intelligence, Surveillance, and Reconnaissance

ISR missions can be conducted with either crewed or uncrewed aircraft. Uncrewed ISR typically uses remotely piloted aircraft (RPA) operated via satellite or data links. Although crewed ISR involves higher costs related to personnel, training, and logistics, it offers greater flexibility, sensitivity, and immediate decision-making [15]. With an effective joint human-AP control mechanism, crewed ISR could be conducted aboard autonomous aircraft when data links are unavailable, retaining these operational advantages.

To the authors' knowledge, no previous work has explored joint human-AP collaboration in the context of crewed ISR. Related works are found in the literature on RPA operations [16], human-AI flight planning [17], and end-to-end mission level autonomy [18].

III. Preliminaries

A. Notation and Main Definitions

For a continuously differentiable function $h : \mathcal{D} \to \mathbb{R}$, $\mathcal{D} \subseteq \mathbb{R}^n$, $\nabla h(x)$ denotes the gradient of h and $\dot{h}(x) = \nabla h(x)^T \dot{x}$ when x is understood to be a function of time $t \in \mathbb{R}$ and $\dot{x}$ denotes derivative of x with respect to time. If S is a set, ∂S denotes the boundary of S. The positive real numbers are denoted $\mathbb{R}_{>0}$, and $\|x\|$ is the standard Euclidean norm of a vector x. A continuous function $\eta : \mathbb{R} \to \mathbb{R}$ is said to be of ***extended class-$\mathcal{K}_\infty$*** if $\eta(0) = 0$, it is strictly increasing, and if $\lim_{s\to\infty} \eta(s) = \infty$.

B. Standard CBFs Formulation

Safety is understood as forward invariance [19, Ch. 4] of a subset of the state space $S = \{x \mid h(x) \geq 0\}$ with respect to a controlled system $\dot{x} = f(x) + g(x)u$, with $x \in \mathcal{D} \subseteq \mathbb{R}^n$, $u \in \mathbb{R}^m$, and f, g locally Lipschitz. $h(x) : \mathcal{D} \to \mathbb{R}$ is said to be a CBF if it satisfies Def. 1.

Definition 1: [20, Def. 2] A continuously differentiable function $h(x) : \mathcal{D} \to \mathbb{R}$, with $S = \{x \mid h(x) \geq 0\}$, is a ***control barrier function*** **(CBF)** for the system $\dot{x} = f(x) + g(x)u$, if there exists an extended class-$\mathcal{K}_\infty$ function η such that for all $x \in \mathcal{D}$

$$\sup_{u \in \mathbb{R}^m} \nabla h(x)^T (f(x) + g(x)u) \geq -\eta(h(x)). \tag{1}$$

Any Lipschitz feedback controller $u(x)$ satisfying (1) for all x guarantees that S is forward invariant. It is common to choose $\eta(h(x)) = \alpha \cdot h(x)$, with $\alpha \in \mathbb{R}_{>0}$.

C. Rate-Tunable CBFs

In contrast to standard CBF theory, [5] proposed treating α as an additional state variable with Lipschitz continuous dynamics. The new system with the extended state is now

$$\begin{bmatrix} \dot{x} \\ \dot{\alpha} \end{bmatrix} = \begin{bmatrix} f(x) + g(x)u \\ f^*(x, \rho) \end{bmatrix} \tag{2}$$

where $f^* : \mathcal{D} \times [-1, 1] \to \mathbb{R}$, $\mathcal{D} \subseteq \mathbb{R}^n$, is Lipschitz continuous and monotonically increasing in ρ, and ρ is a variable that changes over time. The paper [5] uses ρ to model trust among a group of robots, and denotes this new class of CBFs as ***Rate-Tunable CBFs (RT-CBFs)***. In addition, RT-CBFs replace the extended class-$\mathcal{K}_\infty$ function in the right-hand side of (1) by a linear function $\eta(h(x)) = \alpha \cdot h(x)$. More specifically, a continuously differentiable function $h(x) : \mathcal{D} \to \mathbb{R}$ with $S = \{x \mid h(x) \geq 0\}$ is an RT-CBF for the augmented system in (2) and the set S if there exists a compact set $\mathcal{A} \subset \mathbb{R}_{>0}$ such that for all $x \in \mathcal{D}$, $\alpha \in \mathcal{A}$, and $\sup_{u \in \mathbb{R}^m} \nabla h(x)^T (f(x)+g(x)u) \geq -\alpha \cdot h(x)$ holds. Thm. 1 guarantees forward invariance of the safe set S for the system in (2) using RT-CBFs.

Theorem 1: [5, Thm. 1] Consider the augmented system in (2) and a safe set $S = \{x \mid h(x) \geq 0\}$, where h is a RT-CBF. For a locally Lipschitz continuous reference controller $\hat{u} : \mathcal{D} \to \mathbb{R}^m$, let the controller $u = \pi(x, \alpha)$, where $\pi : \mathcal{D} \times \mathbb{R} \to \mathcal{U}$, be formulated as

$$\pi(x, \alpha) = \arg\min_{u \in \mathcal{U}} \|u - \hat{u}(x)\|^2 \tag{3}$$

$$\text{s.t. } \nabla h(x)^T (f(x) + g(x)u) \geq -\alpha \cdot h(x) \tag{4}$$

where $\nabla h(x)$ is also locally Lipschitz continuous. Suppose there exists an upper $\overline{h} > 0$ such that $h(x) < \overline{h}$ for all $x \in S$. Then, the set S is forward invariant.

IV. Attention-Tunable CBFs

In contrast to [5], where trust is obtained geometrically and is a function of both the distance and the angle between autonomous agents, we propose to use instead the human operator's attention level in real time to modify the CBF constraint. We denote this new variant as ***Attention-Tunable CBFs (AT-CBFs)***, a variant of RT-CBFs that relies on the operator's attention level to modify the CBF constraint.

A. Human Attention Metric

The signal $\rho \in \{-1, 1\}$ is constructed by obtaining the Live Area of Interest (LAOI) that the operator is fixated on in the cabin. LAOIs are defined for the ISR Operator Station, the radio communication panel, and for the windows shown in Figure 1. While we considered various eye-tracking metrics, including fixation duration and pupil dilation, we ultimately determined that gaze location provided the most direct measure of attention for our task design. When the operator's gaze is on the Operator Station LAOI, it is assumed that they are attentive and have good SA, so $\rho = 1$. When the operator looks away, $\rho = -1$ and it is assumed that they are not attentive or distracted.

Given the dynamics of α presented in (2), a positive value of $f^*(x, \rho)$ increases the value of α and, as a consequence, relaxes the AT-CBF condition in (4). Otherwise, a negative value decreases α and requires more conservative control actions to satisfy (4). These changes on the conservatism of the AT-CBF directly impact the aircraft's behavior. An increased α allows the aircraft's AP to approach target ships at a faster speed and maneuver closer to them, which we hypothesize will lead to a decrease in mission duration times. From the human perspective, the different values of $f^*(x, \rho)$ are understood as if the AP is aware of when to be more vigilant and self-reliant, or when to rely more on the human.

B. Human Attention Dynamics

Treating α as an additional state variable and extending the state to now include its dynamics allows α to evolve as a continuous function over time, as it is updated every 30 milliseconds, regardless of ρ, the human attention, being detected as a binary variable.

We choose $f^* = \kappa \cdot \beta \cdot \rho$, with $\kappa, \beta \in \mathbb{R}_{>0}$. β corresponds to the fixed value used with standard CBFs and a linear extended class-$\mathcal{K}_\infty$ in the Collision Avoidance behavior. κ is a scaling factor that quantifies how rapidly α changes in each iteration. We limit $\alpha \in [\beta, 100\beta]$, satisfying the requirement for h to be a RT-CBF, with α only taking values in a compact subset $\mathcal{A} \subset \mathbb{R}_{>0}$. For this choice of the lower bound, the AT-CBF is equivalent to the standard CBF, used in the Collision Avoidance mode, at its most conservative behavior, and as the human is attentive to the mission, they are rewarded with a more relaxed constraint. The values of κ and β depend on the experiment design, and in this work they were tuned in pilot experiments based on the testers' feedback during their trials. The nature of human-in-the-loop trials limits the number of runs feasible within this study, thereby constraining our ability to perform exhaustive parameter tuning and comprehensive sensitivity analysis. For all 21 participants, $\kappa = 5$ and $\beta = 0.1$ were used. By normalizing α (i.e. dividing over β), we obtain the operator's accumulated attention during the experiment. Figure 2 validates the choice of $\kappa = 5$ for two participants with very different gaze patterns: participant 08, who spent longer time looking away from the Operator Station LAOI, and participant 17, who looked back and forth between LAOIs more frequently.

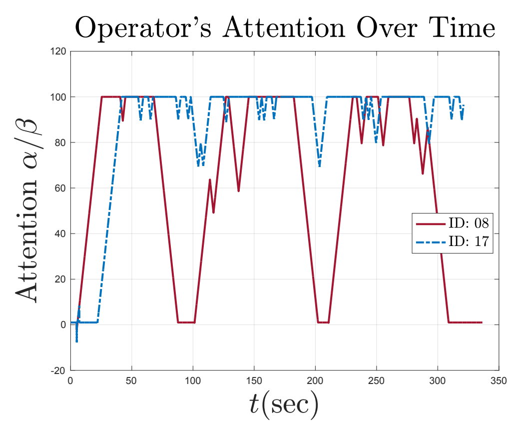

Fig. 2. Attention over time for participants 08 and 17. $\beta \in \mathbb{R}_{>0}$ is the fixed constant for standard CBFs and the lower bound for α with AT-CBFs

In this work, we assume that at each time $t > 0$, there always exists $\alpha \in \mathbb{R}_{>0}$ such that the QP in (3)-(4) remains feasible whenever $h(x) > 0$ and that $\alpha \in \mathcal{A}$. Formally proving that the AT-CBF condition holds uniformly over a compact set is left as future work.

V. ISR Experiment Description

The performance of the AT-CBFs is tested in an updated version of the ISR simulator [6]. The simulator features a full-scale electric vertical takeoff and landing (eVTOL) aircraft cabin. The cabin includes seating with seatbelts, touchscreen interfaces, simulated radio communications equipment, and large windows. Through these windows, participants observe a wall-to-ceiling projection of the external environment provided by Microsoft Flight Simulator. This setup enables high-fidelity immersion while maintaining experimental control, offering a level of realism that goes well beyond typical "game-like" experiences. Figure 3 shows the center panel of the ISR Operator Station user interface. The center panels shows a map of the surveillance area with the position of the user aircraft and the target ships. An alerts panel on the right side of the interface shows messages from the AP to the operator, and a score panel to the left shows time elapsed and damage. The aircraft is modeled as a second order unicycle, as the mission occurs at a constant altitude. The ships are initialized at random positions and do not move. We note that the initial conditions and seeds were selected to be well-separated from constraint boundaries and, in practice, did not lead to infeasibility or multiple simultaneously active constraints during runtime.

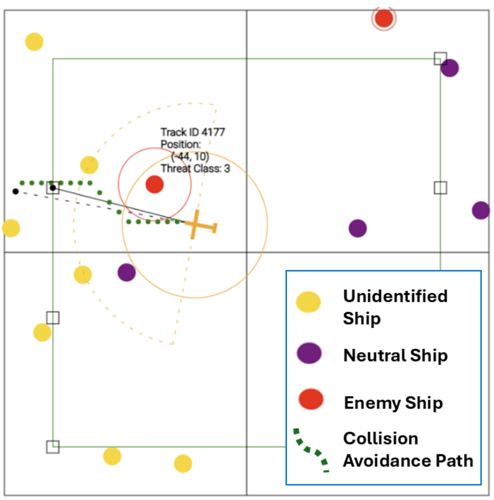

Fig. 3. ISR Operator Station Map. Participants identify ships by overflying them with their long-range sensor (dashed semicircle in front of the aircraft), then classify the ship's weapons by overflying them with the high-resolution sensor (solid circle around the aircraft). In the Collision Avoidance and Adaptive Collision Avoidance behaviors, the AP displays and when necessary intervenes to fly this Collision Avoidance Path that avoids enemy Weapon Engagement Zones.

A. ISR Task

The mission of the joint human-AP team aboard the ISR aircraft is to identify and classify ships in the assigned surveillance area. On the map, unclassified ships are displayed in yellow, neutral ships in purple, and enemy ships in red. The enemy ships have a red circle that represents their WEZ. Once an enemy ship is found, the human must report its ID and the size of its WEZ via radio. At the beginning of the round, all ships are shown as yellow and must be classified by flying within sensor range of the ship. The AP behavior is an independent variable, representing specified combinations of control framework, autonomy, and interaction capabilities:

a) Waypoint: Baseline behavior. The AP defaults to flying a pre-determined navigation pattern but deviates to any arbitrary waypoint input by the operator. Without any operator input and regardless of the position of enemy ships, the AP flies one of two programmed search patterns: 1) Hold which resembles a rectangular orbit or 2) Ladder which stair steps horizontal scans across the surveillance area.

b) Collision Avoidance: In addition to the waypoint behavior, it also includes evasive maneuvers to avoid overflight of enemy WEZs. The AP accepts all operator waypoints as long as they are not inside a WEZ. The Collision Avoidance behavior is implemented using standard CBFs. The CBFs model the WEZ of each enemy according to its position and size, and forces the aircraft controller to avoid overflight of these enemies. However, α is fixed and limits the maximum rate at which the aircraft can approach the WEZs, which can lead to an overly conservative behavior.

c) Adaptive Collision Avoidance: The AP continues its search pattern and proactively executes evasive maneuvers, however, the speed and aggressiveness of the AP continuously adapt to the operator's attention state. The Adaptive Collision Avoidance behavior employs AT-CBFs to create an AP that adapts to the operator's level of attention during the mission.

In this letter, we show how human-autonomy team mission performance (operationalized by aircraft damage and mission duration) can be improved by adapting to the human's real-time physiological state.

B. Experimental Design

The study employs a full factorial within-subjects design with two independent variables: task load (low and high) and AP behavior (Waypoint, Collision Avoidance, and Adaptive Collision Avoidance). At the low task load level, participants face 15 targets in their surveillance area, and the AP flies a simple but less efficient Hold search pattern. At the high task load level, participants face 20 targets and the AP flies a more complicated Ladder search pattern. The Ladder and Hold patterns are based on real-world operational techniques. While the Hold pattern maintains a predictable rectangular orbit, the Ladder pattern involves step-down horizontal sweeps across the surveillance area, enabling broader coverage but requiring increased operator supervision to avoid incurring damage. The selection of 15 and 20 targets to represent low and high task load levels, respectively, was informed by prior studies and further validated by statistically significant differences in workload scores ($p < 0.01$). Balanced Latin Square [21] sequencing is used to minimize learning and other carry-over effects.

Dependent variables include two mission performance metrics: safety (operationalized as aircraft damage) and mission duration. Two additional dependent variables capture the human's physiological state: workload and attention. Workload is measured via the NASA Task Load Index (TLX), a multi-dimensional rating scale that assesses workload based on a weighted average of ratings on six subscales [22]. Finally, we measure human attention using eye gaze, measured with eye-tracking glasses.

C. Participants

The human subjects research protocol was approved by the Georgia Institute of Technology Institutional Review Board. Participants were recruited from the university community and compensated for their time. The results reported in this paper are those of 21 participants (33% female). Five participants had piloting experience (private pilot license or above), and 10 had an undergraduate- or graduate-level AI education. Participants without prior ISR experience were recruited to minimize compensatory strategies and better isolate the effects of AP behavior on mission performance.

Participants were first trained on the ISR simulator, where they were shown a video of the simulator in action, and then given hands-on training. As part of the hands-on training, participants completed two example scenarios: one with the Waypoint AP and a second with the Collision Avoidance AP.

VI. Results

A. Workload

As shown in Figure 4, participants reported higher workload in the high task load scenarios, validating the experimental design. Our NASA TLX analysis used equal weights for each subscale in the composite workload and a scale of 1 to 100. As for AP behaviors, workload was reported in order of highest to lowest as 1) Waypoint, 2) Adaptive Collision Avoidance, 3) Collision Avoidance. Adaptive Collision Avoidance successfully reduces workload as compared to the baseline. However, it still demands more vigilance from the operator than the Collision Avoidance behavior, as expected given the higher speeds and maneuverability of the aircraft. It is unclear if this workload difference would dissipate over time as the crew became more accustomed to the AP behavior.

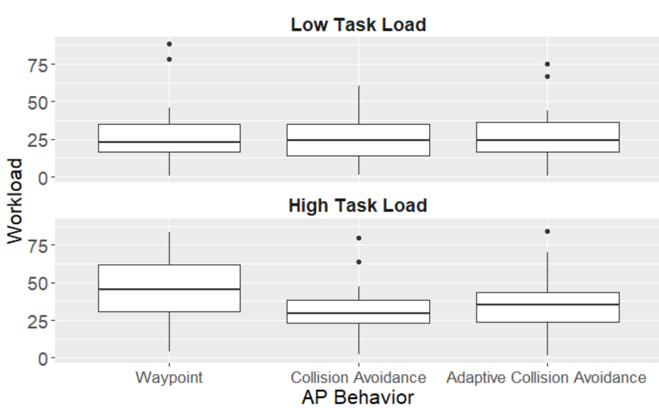

Fig. 4. Distribution of participant composite workload scores for each AP mode, for high and low task load conditions.

The Argus Science ETVision eye tracker recorded measures of pupil diameter, gaze location, and fixation duration. In terms of pupillometry, each participant has a unique physiological baseline, so data were analyzed individually. Pupil dilation has been shown to correlate with increased cognitive workload in aviation contexts [13]. During the study, 19 out of 21 participants experienced an increase in pupil diameter at high task load, also validating our experimental design.

B. Mission Safety

The mission goal is to identify all targets and report all enemy targets, while minimizing damage and in the minimum possible time. This becomes harder to accomplish with the larger number of targets and the more complex search pattern in the high task load scenarios as shown in Figure 5. Figure 5 shows that without any CBF mechanisms, the participants were likely to incur damage, especially in high task load situations. Meanwhile, the standard CBF and AT-CBF mechanisms in the Collision Avoidance and Adaptive Collision Avoidance behaviors almost entirely eliminate aircraft damage. The outlier points correspond to occasions when the participant changed the destination waypoint at the edge of a WEZ boundary at maximum speed. These corner cases caused the quadratic program solver to fail to find a solution to (3), or its CBF equivalent. This is a challenging area for the AP to provide safety in, and it is expected that with experience, operators would learn to exercise caution in these areas of operation. We also note that participants were not provided visual cues of CBFs versus AT-CBFs being active, as we did not want to influence their strategy. Ultimately, it is not possible to guarantee a completely fail-safe system in complex operational representative environments, despite theoretical achievements in simplified environments.

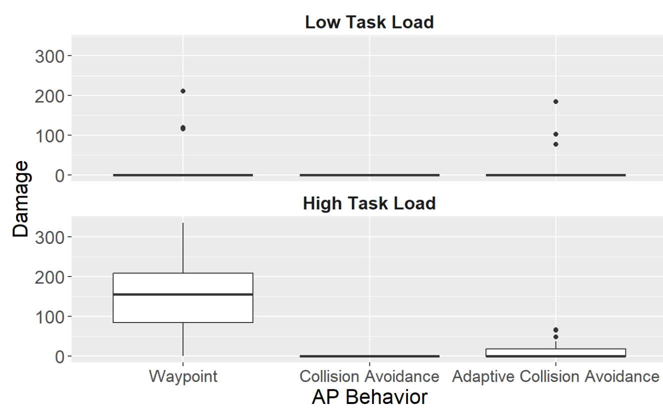

Fig. 5. Distribution of aircraft damage across all participants for each AP mode, for high and low task load conditions.

C. Mission Duration

Figure 6 shows the mission times for each AP behavior for both low and high task load scenarios. For the Waypoint behavior, the mean mission duration was 229.2 seconds, with a median of 217.4 seconds. For the Collision Avoidance behavior, the mean mission duration was 367.4 seconds, with a median of 357.0 seconds. For the Adaptive Collision Avoidance behavior, the mean mission duration was 241.3 seconds, with a median of 223.4 seconds.

A linear mixed-effects model confirmed a statistically significant effect of AP behavior on mission duration ($p < 0.001$). Post hoc pairwise comparisons indicated that mission durations for the Waypoint AP behavior were significantly shorter than those for the Collision Avoidance AP ($p < 0.001$), and Collision Avoidance AP durations were significantly longer than those for the Adaptive Collision Avoidance AP ($p < 0.001$). There was no significant difference in mission duration between Waypoint and Adaptive Collision Avoidance ($p = 0.730$).

Average mission duration was greater under high task load (mean 326.5 seconds, median 311.2 seconds) than low task load (mean 232.1 seconds, median 216.0 seconds). This difference was highly statistically significant according to a Mann-Whitney U test ($W = 853$, $p < 0.001$).

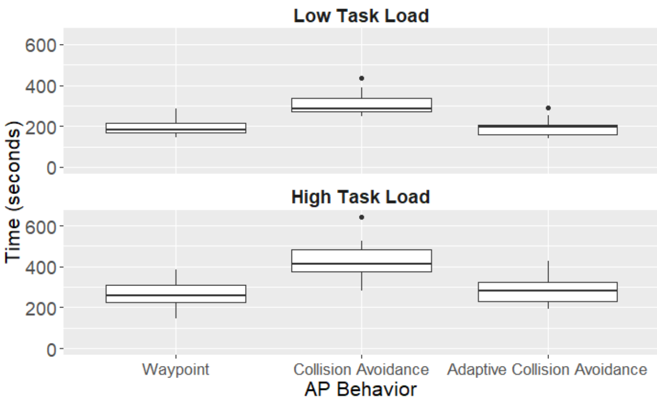

Fig. 6. Distribution of mission duration across all participants for each AP mode, for high and low task load conditions.

VII. Conclusion

Prior studies found that standard CBF controllers improve safety, but worsen mission duration indicating a safety-efficiency trade-off. Working under the premise that automated safety mechanisms are necessary but not sufficient for optimizing human-autonomy team performance [3], we propose a novel formulation of CBFs, Attention-Tunable CBFs, that use real time information of the human onboard in the safety constraint. The results of a human-in-the-loop study with 21 externally recruited participants show that the baseline Waypoint behavior has the fastest mission duration but also greatest risk of aircraft damage. The CBF-based Collision Avoidance behavior improves safety but increases average mission time by 60%. Meanwhile, the AT-CBF-based Adaptive Collision Avoidance behavior mitigates this time-safety trade-off, maintaining the safety of the Collision Avoidance behavior while only increasing the average mission duration by 5% with respect to the baseline.

In conclusion, AT-CBFs enabled safe and efficient jointly controlled ISR by a non-pilot operator teamed with an AP in a specialized aviation mission. This letter shows that it is possible to assure safety while maintaining efficiency of operations. These findings have potentially broad implications for the future of autonomy in and beyond specialized aviation missions. Future work could focus on replacing the binary human attention variable with a more complex metric of attention, using additional physiological measures.

References

[1] "Urban air mobility (UAM) concept of operations version 2.0," Federal Aviation Administration, Tech. Rep., May 2023. [Online]. Available: https://www.faa.gov/air-taxis/uam_blueprint

[2] Airforce Technology, "Collaborative combat aircraft (CCA), USA," https://www.airforce-technology.com/projects/collaborative-combat-aircraft-cca-usa/, 2024.

[3] R. Agbeyibor, V. Ruia, J. Kolb, C. J. Cortes, S. Coogan, and K. M. Feigh, "Towards safe collaboration between autonomous pilots and human crews for intelligence, surveillance, and reconnaissance," in *2024 AIAA DATC/IEEE 43rd Digital Avionics Systems Conference (DASC)*. IEEE, 2024, pp. 1–8.

[4] A. D. Ames, J. W. Grizzle, and P. Tabuada, "Control barrier function based quadratic programs with application to adaptive cruise control," in *53rd IEEE Conference on Decision and Control*. IEEE, 2014, pp. 6271–6278.

[5] H. Parwana, A. Mustafa, and D. Panagou, "Trust-based rate-tunable control barrier functions for non-cooperative multi-agent systems," in *2022 IEEE 61st Conference on Decision and Control (CDC)*. IEEE, 2022, pp. 2222–2229.

[6] R. Agbeyibor, V. Ruia, J. Kolb, and K. M. Feigh, "Joint intelligence, surveillance, and reconnaissance mission collaboration with autonomous pilots," in *Proceedings of the Human Factors and Ergonomics Society Annual Meeting*, vol. 68, no. 1, 2024, publisher: SAGE Publications Inc.

[7] A. D. Ames, X. Xu, J. W. Grizzle, and P. Tabuada, "Control barrier function based quadratic programs for safety critical systems," *IEEE Transactions on Automatic Control*, vol. 62, no. 8, pp. 3861–3876, 2016.

[8] J. Kim, J. Lee, and A. D. Ames, "Safety-critical coordination for cooperative legged locomotion via control barrier functions," in *2023 IEEE/RSJ International Conference on Intelligent Robots and Systems (IROS)*. IEEE, 2023, pp. 2368–2375.

[9] X. Tan and D. V. Dimarogonas, "Distributed implementation of control barrier functions for multi-agent systems," *IEEE Control Systems Letters*, vol. 6, pp. 1879–1884, 2021.

[10] K. M. Feigh and A. R. Pritchett, "Requirements for effective function allocation: A critical review," *Journal of Cognitive Engineering and Decision Making*, vol. 8, no. 1, pp. 23–32, March 2014.

[11] N. Liang, J. Yang, D. Yu, K. O. Prakah-Asante, R. Curry, M. Blommer, R. Swaminathan, and B. J. Pitts, "Using eye-tracking to investigate the effects of pre-takeover visual engagement on situation awareness during automated driving," *Accident Analysis & Prevention*, vol. 157, p. 106143, July 1 2021. [Online]. Available: https://doi.org/10.1016/j.aap.2021.106143

[12] C. Ahlström, K. Kircher, M. Nyström, and B. Wolfe, "Eye tracking in driver attention research—how gaze data interpretations influence what we learn," *Frontiers in Neuroergonomics*, vol. 2, December 8 2021. [Online]. Available: https://doi.org/10.3389/fnrgo.2021.778043

[13] G. Ziv, "Gaze behavior and visual attention: A review of eye tracking studies in aviation," *The International Journal of Aviation Psychology*, vol. 26, no. 3–4, pp. 75–104, October 1 2016. [Online]. Available: https://doi.org/10.1080/10508414.2017.1313096

[14] T. Louw and N. Merat, "Are you in the loop? using gaze dispersion to understand driver visual attention during vehicle automation," *Transportation Research Part C: Emerging Technologies*, vol. 76, pp. 35–50, March 1 2017. [Online]. Available: https://doi.org/10.1016/j.trc.2017.01.001

[15] (2023) U.s. air force doctrine 2-0 intelligence. [Online]. Available: https://www.doctrine.af.mil/

[16] D. Roza. AFSOC flies 3 reapers with one crew in first-of-its-kind exercise. [Online]. Available: https://www.airandspaceforces.com/afsoc-multiple-mq-9-reapers/

[17] L. M. Xie, E. Conway, H. Cheng, and F. Amsaad, "Exploration of Multi-Agent Reinforcement Learning for ISR Flight Path Planning," in *NAECON 2024 - IEEE National Aerospace and Electronics Conference*, Jul. 2024, pp. 328–333, iSSN: 2379-2027. [Online]. Available: https://ieeexplore.ieee.org/abstract/document/10670352

[18] T. Uhm, J.-W. Lee, G.-T. Kim, S.-G. Yang, J.-Y. Kim, J.-K. Kim, and S. Kim, "Decision-Making System of UAV for ISR Mission Level Autonomy," *Journal of the Korean Society for Aeronautical & Space Sciences*, vol. 49, no. 10, pp. 829–839, 2021, publisher: The Korean Society for Aeronautical and Space Sciences. [Online]. Available: https://www.koreascience.or.kr/article/JAKO202128837645003.view

[19] H. K. Khalil, *Nonlinear systems; 3rd ed.* Prentice-Hall, 2002.

[20] A. D. Ames, S. Coogan, M. Egerstedt, G. Notomista, K. Sreenath, and P. Tabuada, "Control barrier functions: Theory and applications," in *2019 18th European control conference (ECC)*. IEEE, 2019, pp. 3420–3431.

[21] J. V. Bradley, "Complete counterbalancing of immediate sequential effects in a latin square design," *Journal of the American Statistical Association*, vol. 53, no. 282, pp. 525–528, 1958.

[22] S. G. Hart, "Nasa task load index (tlx)," January 1986. [Online]. Available: https://ntrs.nasa.gov/citations/20000021487